Karlsruher Institut für Technologie

FAKULTÄT FÜR PHYSIK

PHYSIKALISCHES PRAKTIKUM FÜR FORTGESCHRITTENE

PRAKTIKUM MODERNE PHYSIK

Gruppe Nr. _____ Kurs: **Mo1** **Mo2** **Mi3**

zutreffendes bitte ankreuzen

aktuelles Semester angeben

Versuch: _____

Namen: _____

_____

Assistent: _____

durchgeführt am: _____

Protokollabgabe am: _____

_____

vom Betreuer auszufüllen

Note gesamt [+] [0] [-]

Anerkannt: _____

(Datum Unterschrift)

Datum Rückgabe: _____

Bemerkung:

Contents

List of Figures

1. Introduction

This lab report covers the analysis and interpretation of data taken at the LHC by the CMS Collaboration in 2010. The data-set was pre-processed to contain only information about two well reconstructed muon events for the use of this lab course. The analysis covers the determination of various event parameters with an emphasis on the dimuon spectrum and the Z boson. If not specified further, every information is aquired from the given literature [1].

1.1 CMS and Muon Detection

In order to detect muons at the LHC, the CMS detector is designed as an onion-like arrangement of detectors. From the inside CMS is built of a silicon-based trace detector, an electromagnetic calorimeter, a hadronic calorimeter, solenoid magnets and the muon chambers, a cross-section can be seen in figure 1.1. Each layer is able to measure different parameters, such that a wide range of different particles can be measured. Due to their minimal ionizing behavior, muons are only detected by the inner tracker and the muon system in the last shell. By combining the data taken by these two detectors, muon tracks are reconstructed. The transverse momentum resolution then depends on the detector geometry.

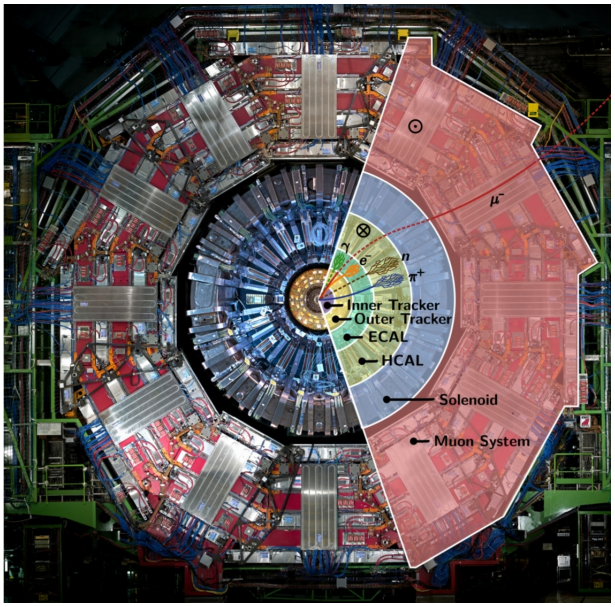

Figure 1.1: Cross-section of the CMS detector system picturing the different detector shells. Particles are depicted in continuous lines in parts that can detect them and in interrupted lines wherever they cannot be detected.

To analyze certain events within CMS, the quantities rapidity y and pseudorapidity η are introduced based on the experiments geometries. By establishing the x-axis as horizontal, pointing towards the center of the LHC, the y-axis as vertical upwards and the z-axis west along the beam line. The angle between the y- and z-axis is referred to as θ and the angle between y- and x-axis as ϕ. Rapidity and pseudorapidity are defined as

$$y = \frac{1}{2} ln \left(\frac{E + p_z}{E - p_z} \right), \tag{1.1}$$

$$\eta = \frac{1}{2} ln \left(\frac{|\overrightarrow{p}| + p_z}{|\overrightarrow{p}| - p_z} \right). \tag{1.2}$$

For high energies the pseudorapidity can be rewritten as

$$\eta = -ln \left(tan \frac{\theta}{2} \right). \tag{1.3}$$

Since the transversal momentums role in the initial proton-proton collision is negligible, the resulting transverse impulse of a collision event has to be preserved. The transverse impulse p_T is used in addition to rapidity or pseudorapidity and ϕ in order to describe decay products of the collision. By reconstruction of the original particle, the invariant mass M can be calculated as

$$M = \sqrt{\sum_i P_i} = \sqrt{(E_1 + E_2)^2 - (p_{x,1} + p_{x,2})^2 - (p_{y,1} + p_{y,2})^2 - (p_{z,1} + p_{z,2})^2}, \tag{1.4}$$

with the four-vectors of the corresponding decay products. While the rapidity and invariant mass are Lorentz invariant, pseudorapidity in the case of 1.3 is independent of particle mass, such that the spatial distance between two particles,

$$\Delta R = \sqrt{(\Delta\eta)^2 + (\Delta\phi)^2}, \tag{1.5}$$

can be introduced.

1.2 Dimuon Spectrum

When observing decays that lead to muon final states, a muon and anti-muon pair resulting from the decay of one particle is referred to as a dimuon pair. From detection of the energy and momentum of the resulting muon final states, the invariant mass of the original particle can be reconstructed. The dimuon spectrum, shown in figure 1.2, shows the distribution of the invariant mass of dimuon pairs.
The resonances in the dimuon spectrum can be described by Voigt distributions, with decay widths Γ and certain life times τ. Γ is given by the resonances' half-width and can be obtained by a fit of the resonances. τ is defined as the time in which the number of studied particles in a system drops to $\frac{1}{e}$ times its original size. These quantities are related through the uncertainty relation, they can be described in neutral units as

$$\Gamma = \frac{1}{\tau}. \tag{1.6}$$

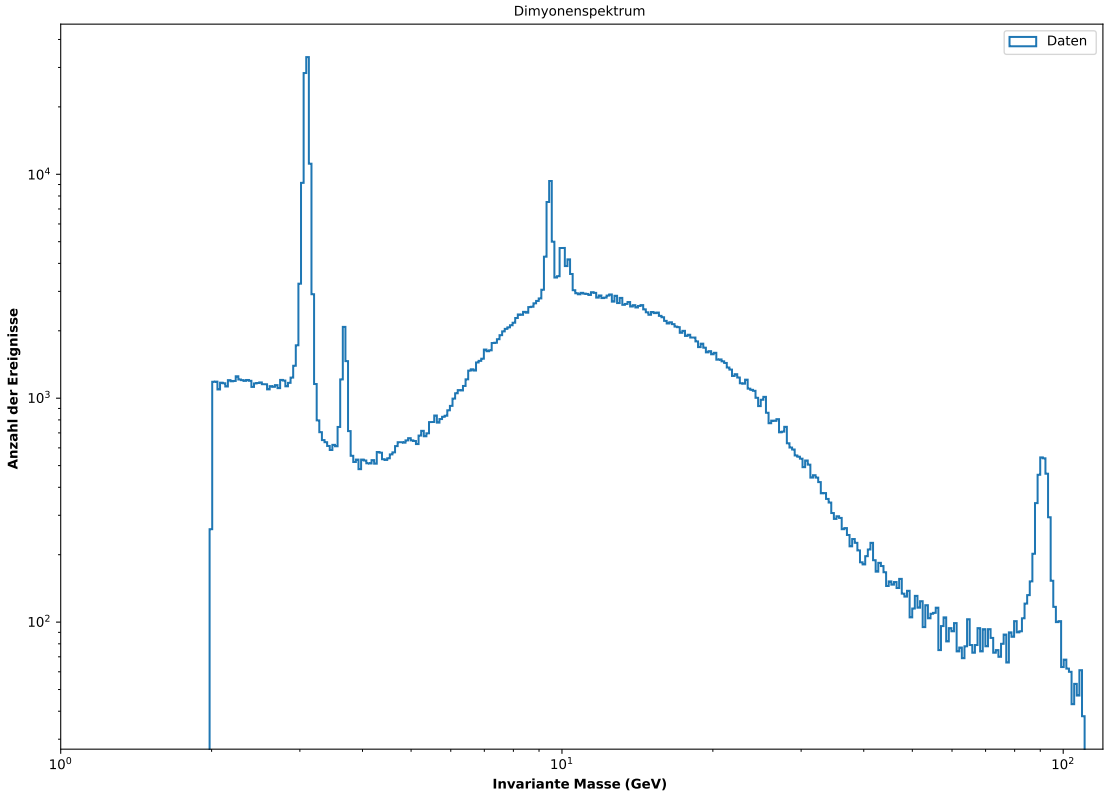

Figure 1.2: Whole Dimuon spectrum of the analyzed data. The plot shows the number of events over the invariant mass of the dimuon pairs, as well as labeled resonances.

The Voigt distribution,

$$V(x) = (G * B)(x) = \int G(\tau)L(x-\tau)d\tau \tag{1.7}$$

is a convolution of a Gaussian,

$$G(x) = \frac{1}{\sigma\sqrt{2\pi}} exp\left(-\frac{1}{2}\frac{(x-M)^2}{\sigma^2}\right), \tag{1.8}$$

with standard deviation σ and mean M, and a Breit-Wigner distribution,

$$B(x) = \frac{\frac{\Gamma}{2}}{\pi\left((x-M)^2 + (\frac{\Gamma}{2})^2\right)}. \tag{1.9}$$

1.3 Z Boson and J/Ψ Meson

Z bosons are created through quark-antiquark or lepton-antilepton pair reactions and has a $(3.366 \pm 0.007)\%$ probability to decay into a dimuon pair. The Z bosons life time and effective cross section regarding the decay into a dimuon pair is

$$\tau_Z = (2.6378 \pm 0.0024 \cdot 10^{-25})\text{s}, \tag{1.10}$$

$$\sigma_{Z\to\mu\mu} = (0.968 \pm 0.008\ (\text{stat.})\ \pm 0.007\ (\text{syst.})\ \pm 0.018\ (\text{th.})\ \pm 0.039\ (\text{lumi.}))\text{nb}. \tag{1.11}$$

The J/Ψ Meson is the bound state of a charm and anticharm quark pair, also referred to as 'charmonium', with the lowest energy. It has an about 6 % chance to decay into dielectron or dimuon pair. Both particles are well known, with masses and decay widths

$$M_Z = (91.1876 \pm 0.0021)\text{GeV}, \tag{1.12}$$
$$\Gamma_Z = (2.4952 \pm 0.0023)\text{GeV}, \tag{1.13}$$
$$M_{J/\Psi} = (3096.900 \pm 0.006)\text{MeV}, \tag{1.14}$$
$$\Gamma_{J/\Psi} = (92.9 \pm 2.8)\text{keV}. \tag{1.15}$$

The Z boson is often used for energy calibration of detectors. The very short decay width of the J/Ψ meson makes it a convenient standard candle to be used in determination of detector resolution.
Because of the high mass of the Z boson it can only be formed by two high energy partons that therefore cannot have a big difference in momentum. The J/Ψ meson, having around 3.5 % of the Z bosons' mass, doesn't require high energy partons, such that the momentum difference of the colliding partons can be big. This results in a wider opening angle for the decay products of the Z boson than for those of the J/Ψ meson, since the partons associated with the J/Ψ meson are accelerated significantly more along the beam axis than the of the Z boson. Additionally, the decay products of the J/Ψ meson have less momentum and transverse momentum since the J/Ψ meson has less rest energy to distribute onto its decay products.

2. Data Analysis

In the course of evaluating dimuon events, two candidates originating in a Z boson and two originating in a J/Ψ meson have been documented, as seen in figure 2.1 and 2.2. The Z boson events are primarily chosen because of the wide angle between the decay products, as elaborated in the previous chapter. The J/Ψ meson events show a smaller angle between decay products and slightly curved trajectories due to the increased acceleration along the beam axis. Also the muons resulting from the Z boson decay leave a slightly longer trail in the detector system, as the Z boson can provide more energy to it's decay products than the J/Ψ meson.

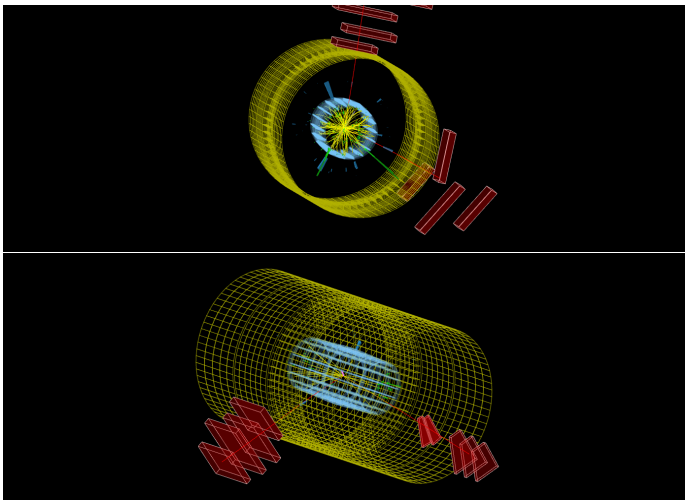

Figure 2.1: Two different possible Z boson events

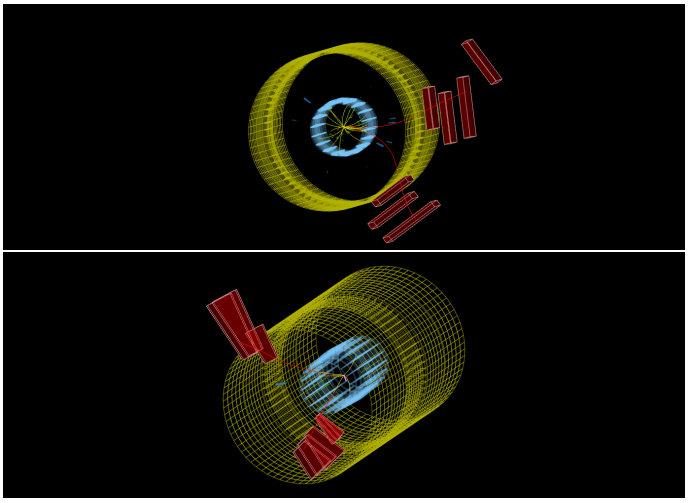

Figure 2.2: Two different possible J/Ψ meson events

2.1 Analysis for the Determination of M_Z, Γ_Z, τ_Z, $\sigma_{Z\to\mu\mu}$

In order to calculate M_Z, Γ_Z, τ_Z and $\sigma_{Z\to\mu\mu}$ the general distributions of the provided data-set are investigated before the Z boson peak is analyzed. For the latter analysis the sidebands of the Z boson peak are used to determine a background parameterization and the detector resolution is computed by analysis of the sharp J/Ψ peak.
First the quantities established in chapter 1.1 are computed. The therewith calculated invariant mass in accordance to the number of events results in the dimuon spectrum displayed in figure 1.2. Pseudorapidity, azimuthal angle Φ, transversal impulse as well as ΔR, ΔΦ and $\Delta\eta$ have been determined for three cases, one including the whole mass range with invariant mass 1 to 120, one covering the estimated J/Ψ invariant mass range from 2.8 to 3.4 and one the range around the Z boson peak from 60 to 110. The results are shown in figures 2.3, 2.4 and 2.5.

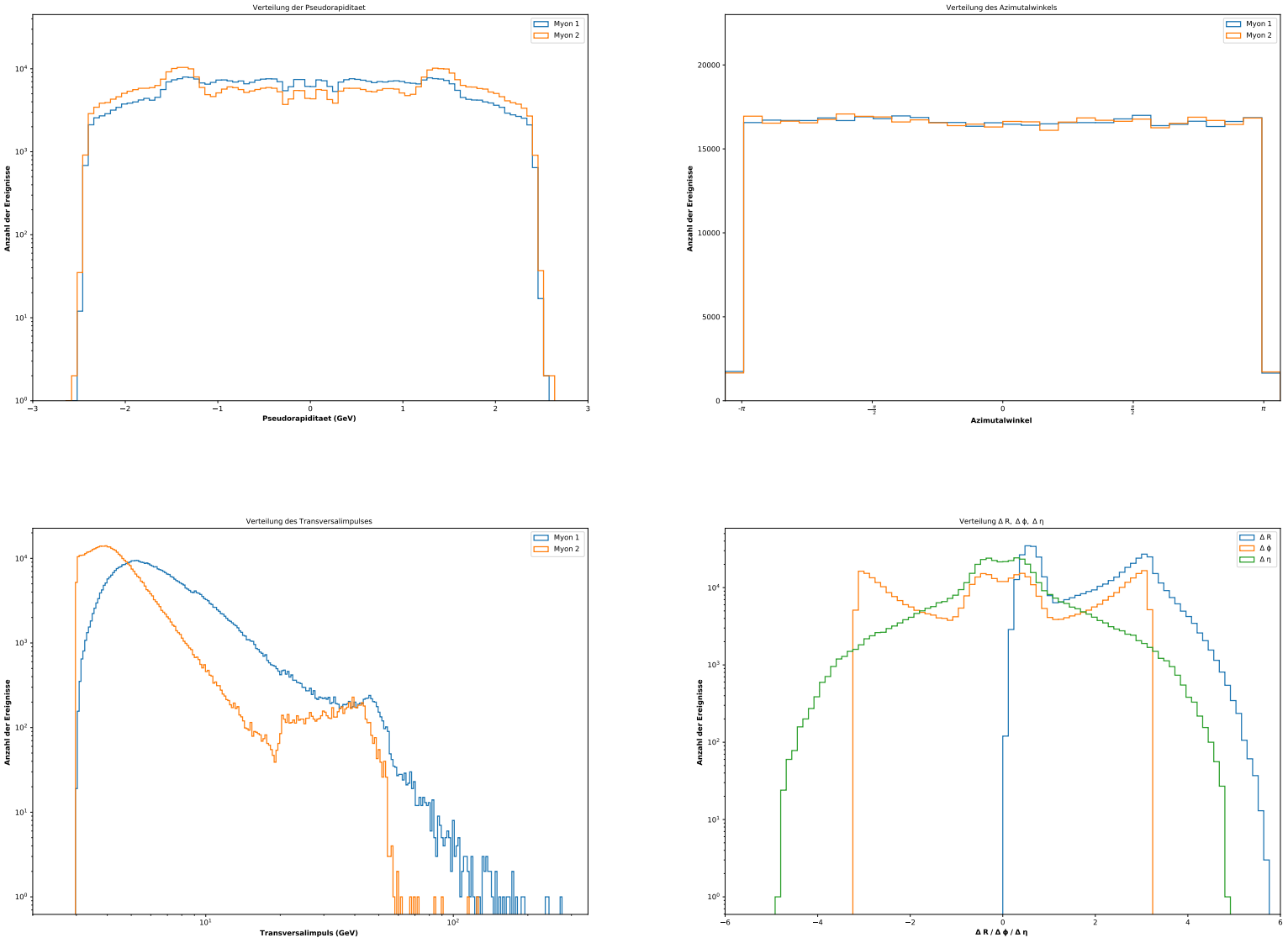

Figure 2.3: Psuedorapidity, the azimuthal angle Φ, transverse impulse p_T as well as ΔR, ΔΦ and $\Delta\eta$ distributions in accordance to the number of events for the whole invariant mass range.

In figure 2.4 the distribution of pseudorapidity shows a peak around 0. This is in accordance with the pseudorapidity estimation for high energies and the transversal impulse, which is bigger then the one corresponding to the J/Ψ meson displayed in figure 2.5. The Pseudorapidity in figure 2.5 is therefore symmetrically distributed in two peaks left and right of the minimum at 0. The distribution of azimuthal angle Φ also fits the expectation of bigger angles between the decay products of the Z boson and evenly distributed angles between the decay products of the J/Ψ meson. This is in accordance with the differences of location ΔR, azimuthal angle ΔΦ and pseudorapidity $\Delta\eta$ shown in the lower right graphs. It's displaying low differences for the J/Ψ meson because of the small transversal momentum and big differences for the Z boson, while the pseudorapidity still centers around 0.

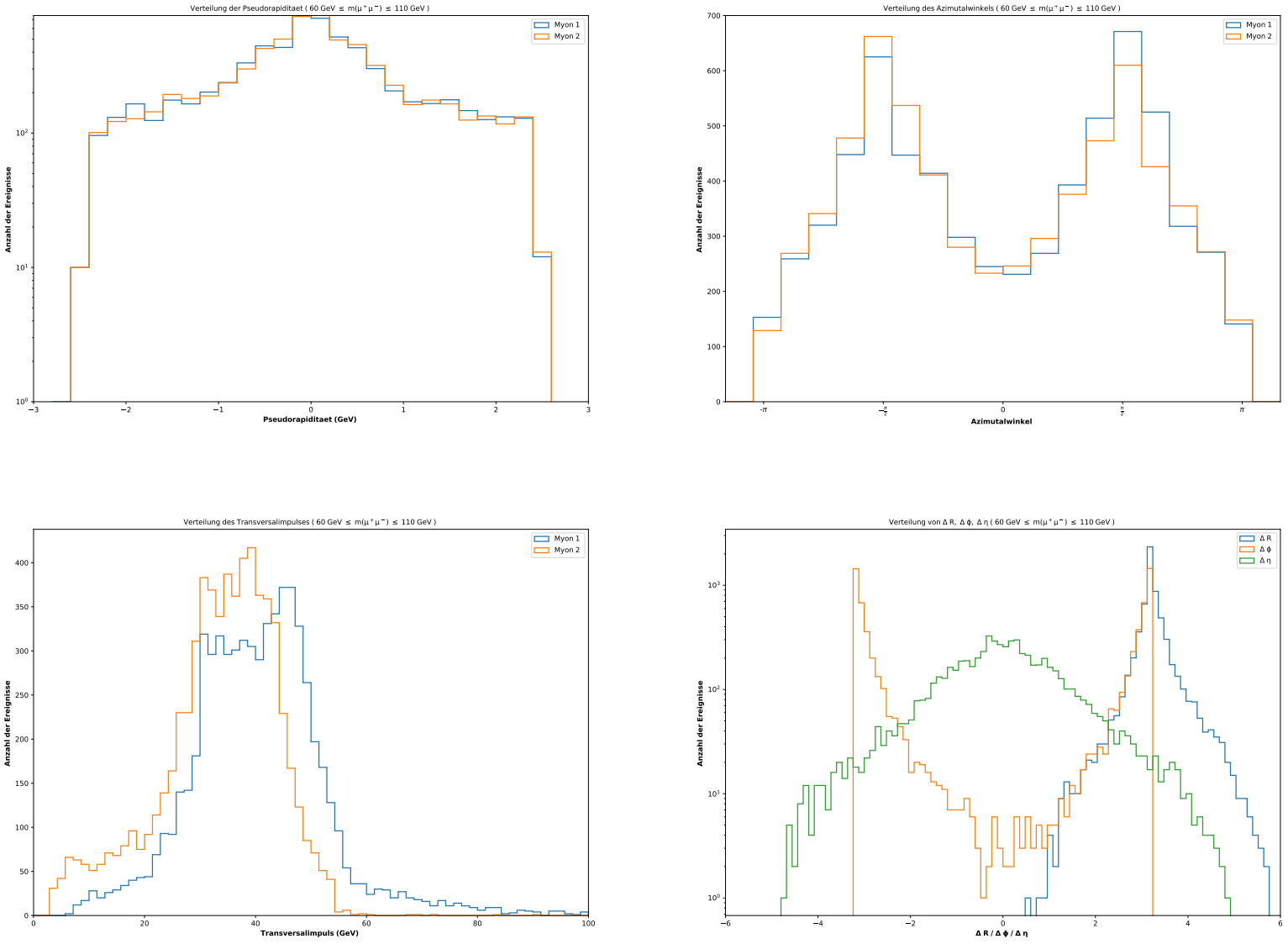

Figure 2.4: Psuedorapidity, the azimuthal angle Φ, transverse impulse p_T as well as ΔR, ΔΦ and $\Delta\eta$ distributions in accordance to the number of events for the Z boson invariant mass range.

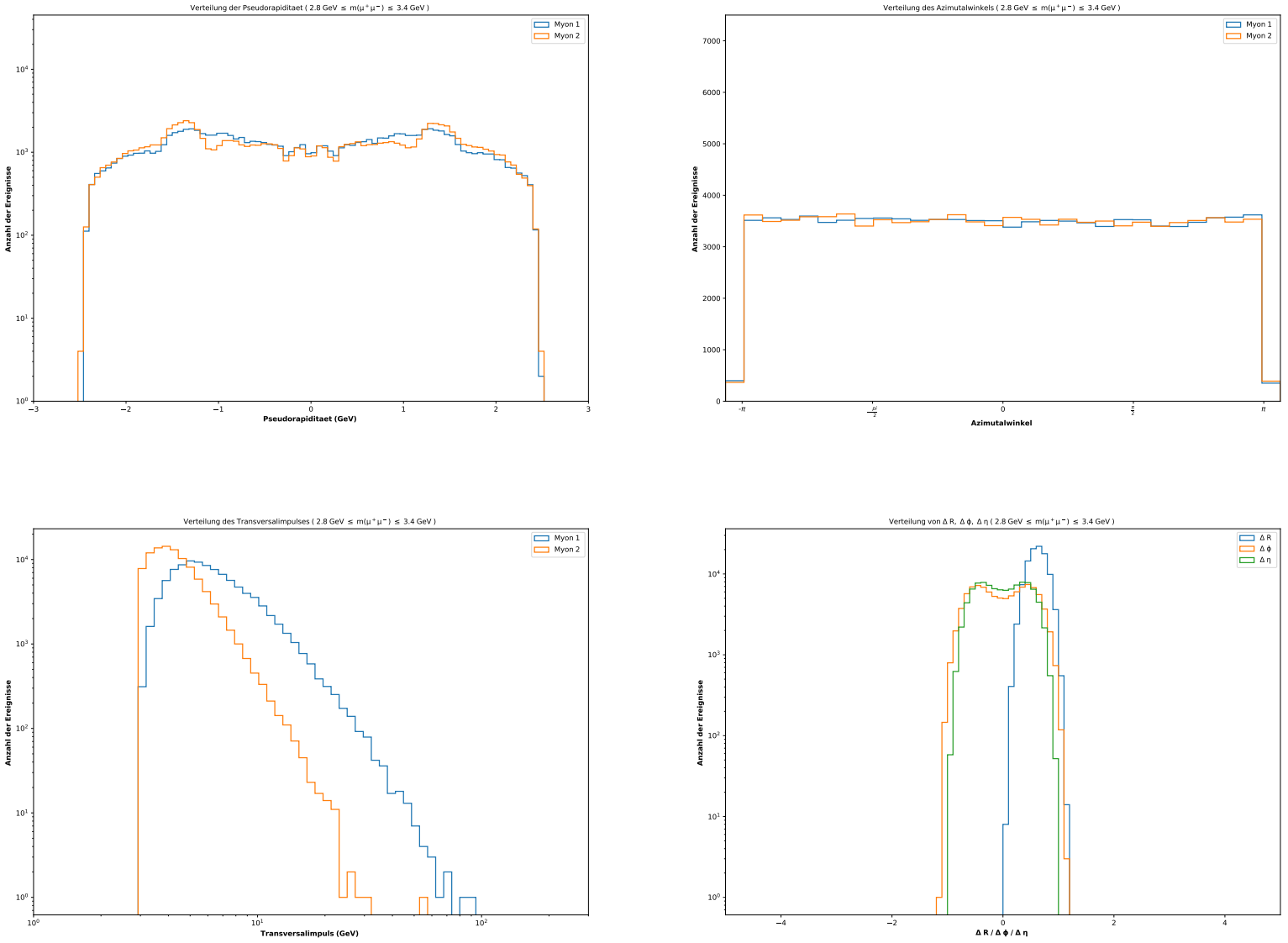

Figure 2.5: Psuedorapidity, the azimuthal angle Φ, transverse impulse p_T as well as ΔR, $\Delta\Phi$ and $\Delta\eta$ distributions in accordance to the number of events for the J/Ψ meson invariant mass range.

2.1.1 Investigating the Z boson peak

To further analyze the Z boson peak, the peak itself as well as the sideband regions are examined seperatly in order to isolate background and signal. The sideband region is then used for a background parameterization and the signal region is fitted according to the Voigt distribution as introduced in equation 1.7. The spectrum around the peak, the isolated sideband regions and the transversal impulse around the signal are shown in figure 2.6.

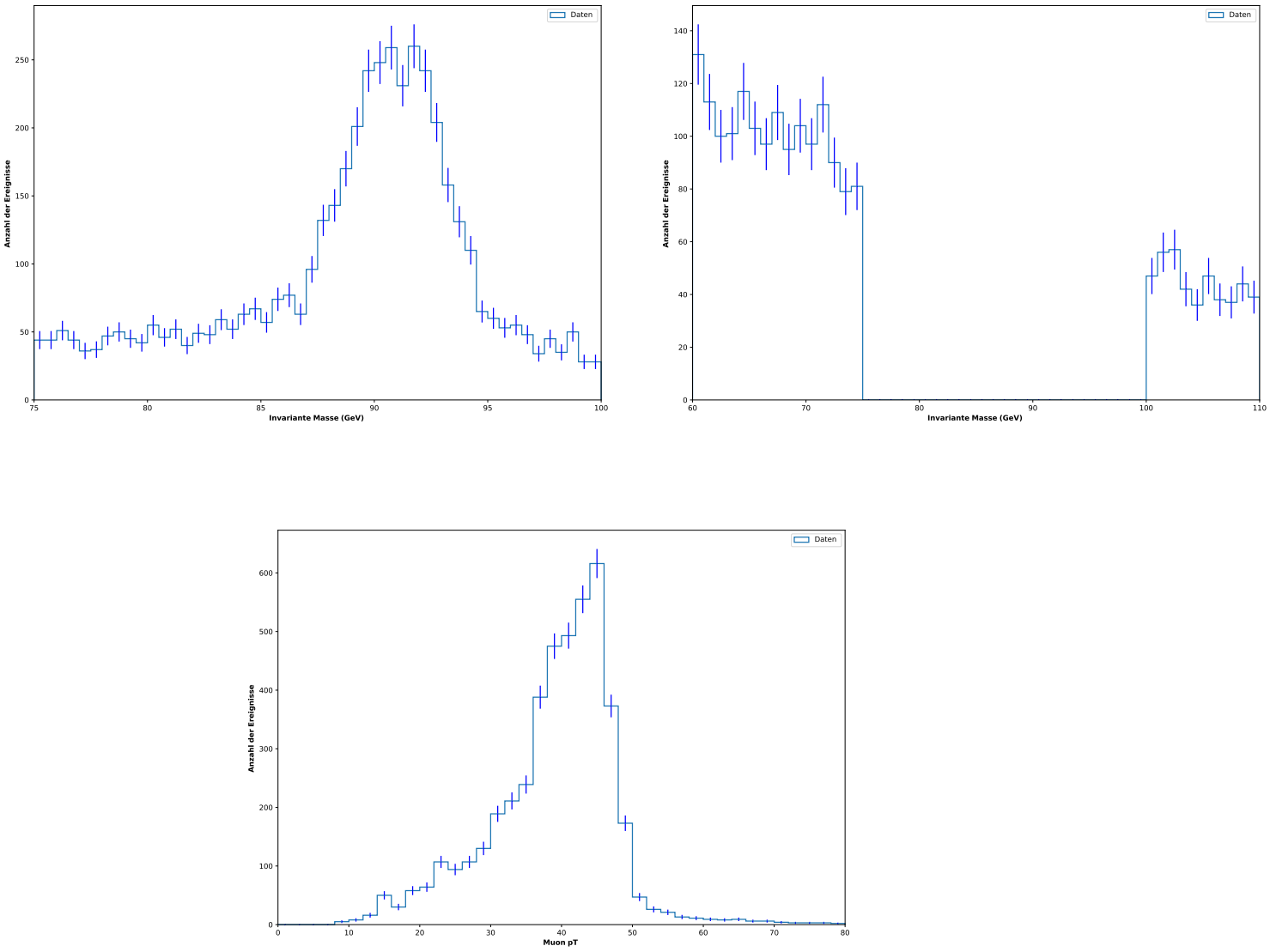

Figure 2.6: Spectrum around the peak, the isolated sideband regions and the transversal impulse around the signal. The error bars represent the corresponding Poisson errors.

Determination of a Backgrond parameterization

To determine the parameterization of the background, the sideband region is fitted with different legendre polynomials of degree 0 to 5. In order to perform a smoother fitting procedure, the background data was binned. Afterwards a comparison of $\frac{\chi^2}{NDF}$, with NDF representing the number of degrees of freedom, is done to chose the best polynomial fit. A fit is optimal with $\frac{\chi^2}{NDF} \approx 1$. All performed fits are shown in figure 2.7, where a comparison shows that $|\frac{\chi^2}{NDF} - 1|$ is minimal with a legendre polynomial of degree 5.

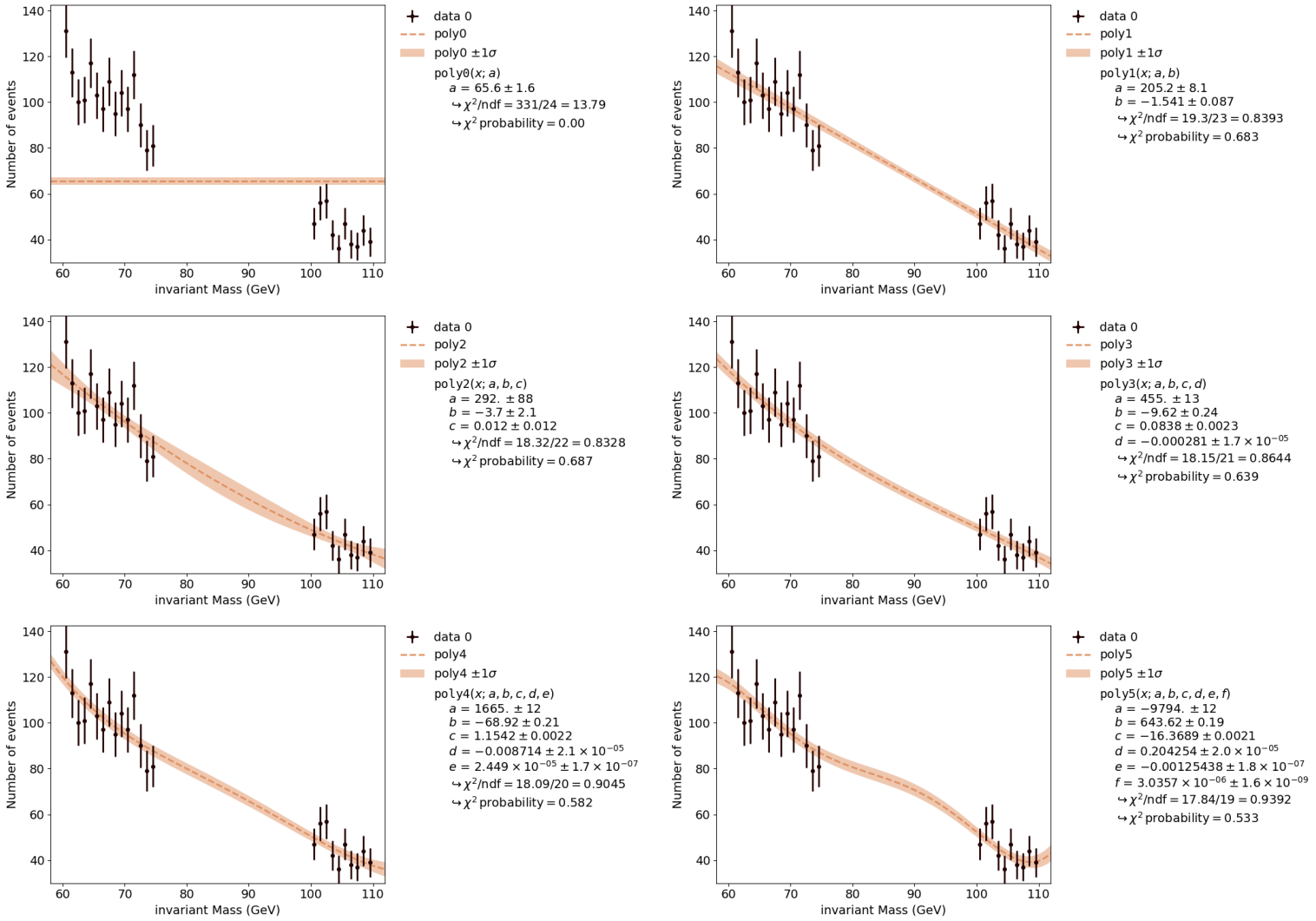

Figure 2.7: Fit of the sideband regions with different polynomials to compare $\frac{\chi^2}{NDF}$.

2.1.2 Estimation of the Detector Resolution

Since the J/Ψ meson peak is very sharp and has a long lifetime because of the suppression of hadronic decays due to the OZI rule, it's Breit-Wigner width Γ can be neglected, such that it can be used to determine the Gaussian fraction of the final Voigtian distribution by computing the width of the resonance. In order to obtain a more accurate result the data was binned in different p_T bins and multiple values of the muon momentum resolution where calculated. To determine the mass resolution the function is extrapolated to the region of the Z boson and the mass resolution obtained via the relation

$$\frac{\Delta M}{M} = \frac{\Delta p_T}{p_T}. \tag{2.1}$$

The extrapolation of the linear resolution function can be seen in figure 2.8. The resulting impulse resolution can be seen in figure 2.9. Because of the strong correlation of Γ_z and σ_z, the latter is introduced to the fit as a constraint and is estimated.

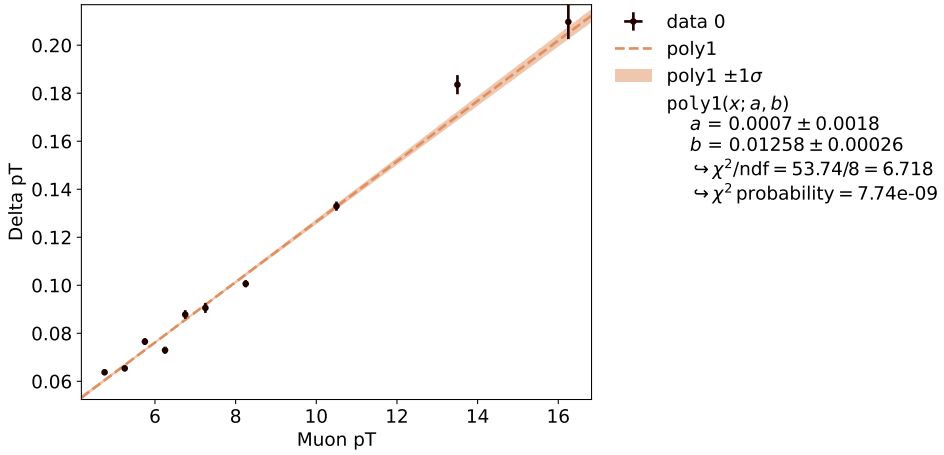

Figure 2.8: Extrapolation of the linear resolution function from the J/Ψ resonance.

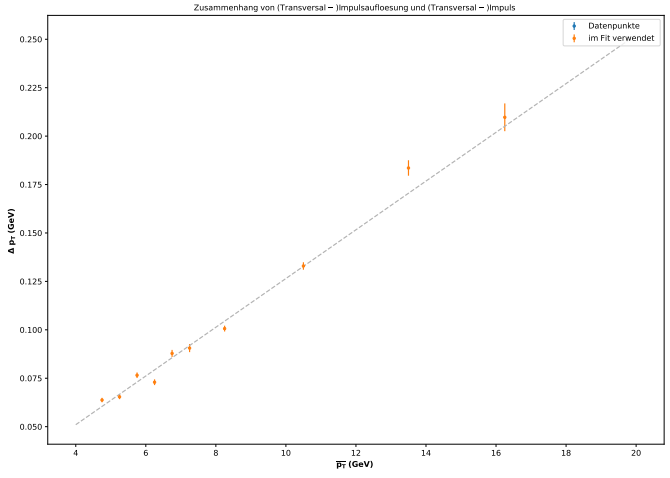

Figure 2.9: Resulting transversal impulse resolution.

2.1.3 Concluding Obtained Background and Resolution Data Into Model Fit

According to the bins chosen for the transversal momentum before, the final fit is performed by dividing the data set into different p_T regions, where the corresponding mass resolution is used in each region, to model the mass resolution more realistically. The fits where then performed with the python package Kafe2 multifit option and input parameters $\mu = 91$ as well as $\Gamma = 2.5$, including the background parameterization and estimated detector resolution. The signal fit is displayed in figure 2.10 and the background fit in figure 2.11. The resulting values for Z boson mass, decay width, lifetime and cross section are

$$M_Z = (90.874 \pm 0.065)\text{GeV}, \tag{2.2}$$
$$\Gamma_Z = (1.891 \pm 0.074)\text{GeV}, \tag{2.3}$$
$$\tau_Z = \frac{1}{\Gamma_Z} = (0.529 \pm 0.002)\text{GeV}^{-1} = (3.486 \pm 0.013) \cdot 10^{-25}\text{s}, \tag{2.4}$$
$$\sigma_{Z->\mu\mu} = (1.12 \pm 0.25)\text{nb}. \tag{2.5}$$

Compared with literature these values show deviations of

$$\Delta M_Z \approx 0.3\,\%, \tag{2.6}$$
$$\Delta \Gamma_Z \approx 24.21\,\%, \tag{2.7}$$
$$\Delta \tau_Z \approx 32.16\,\%, \tag{2.8}$$
$$\Delta \sigma_{Z->\mu\mu} \approx 15.7\,\%. \tag{2.9}$$

Here M_Z and $\sigma_{Z->\mu\mu}$ lie within the error margins of the literature. The difference of Γ_z with its corresponding literature value is quite high, which may result from the estimation of detector resolution. An optimization could be made regarding the chosen regions of invariant mass, as well as the chosen sideband and signal regions for the Z boson and J/Ψ meson peaks.

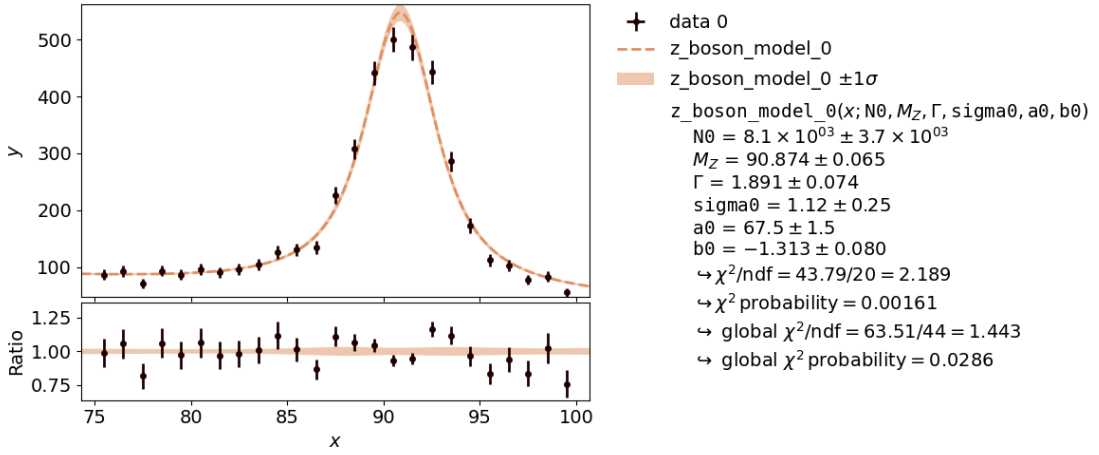

Figure 2.10: Kafe2 signal multifit with output parameters.

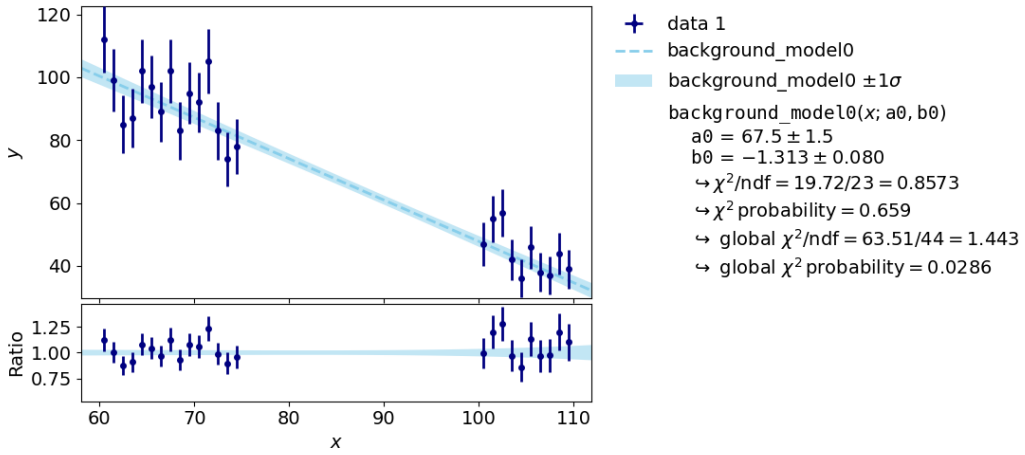

Figure 2.11: Kafe2 background multifit with output parameters.

Bibliography

[1] given Literature